TELKOMNIKA Telecommunication Computing Electronics and Control
Vol. 22, No. 5, October 2024, pp. 1257~1268
ISSN: 1693-6930, DOI: 10.12928/TELKOMNIKA.v22i5.25834

Study of ISFET sensitivity to pH variations using Silvaco TCAD

Nur Afiqah Hani Senin[1], Anis Suhaila Mohd Zain[1], Fauziyah Salehuddin[1], Hazura Haroon[1], Ahmed Musa Dinar[2], Norwahidah Abdul Karim[3]
[1]Department of Computer Engineering, Faculty of Electronics and Computer Technology and Engineering, Universiti Teknikal Malaysia Melaka, Melaka, Malaysia
[2]Department of Computer Engineering, University of Technology–Iraq, Baghdad, Iraq
[3]Department of Biochemistry, Faculty of Medicine, Universiti Kebangsaan Malaysia, Kuala Lumpur, Malaysia

Article Info

Article history:

Received Oct 31, 2023
Revised May 17, 2024
Accepted May 26, 2024

Keywords:

Electrolyte
High-k materials
Ion-sensitive field-effect transistor
pH sensitivity
Silvaco technology computer-aided design

ABSTRACT

Chemical sensors are increasingly used in healthcare because of their small size, durability, low resistance, and quick reaction time. This research aims to develop a pH biosensor utilizing an ion-sensitive field-effect transistor (ISFET) simulated with Silvaco technology computer-aided design (TCAD) software. The pH range of operation for the ISFET is 2 to 12. Sensitivity was evaluated based on the critical pH value and threshold voltage (V_{th}) parameters across different gate channel lengths (250 nm, 200 nm, and 50 nm) and sensing membrane thicknesses (3 nm, 10 nm, and 20 nm). The sensitivity of different materials to pH levels was measured. Titanium dioxide (TiO_2) had the highest sensitivity at 57.98 mV/pH, followed by hafnium (IV) oxide (HfO_2) at 57.46 mV/pH, tantalum pentoxide (Ta_2O_5) at 57.36 mV/pH, aluminium oxide (Al_2O_3) at 55.05 mV/pH, and silicon nitride (Si_3N_4) at 54.75 mV/pH. Notably, TiO_2 with a 200 nm gate channel length and a 3 nm sensing membrane thickness demonstrated the highest sensitivity. These findings highlight the potential of ISFETs, particularly those with TiO_2 sensing membranes, as robust and precise pH monitoring platforms in the biomedical industry.

Corresponding Author:

Anis Suhaila Mohd Zain
Department of Computer Engineering, Faculty of Electronics and Computer Technology and Engineering
Universiti Teknikal Malaysia Melaka
Jalan Hang Tuah, 76100, Durian Tunggal, Melaka, Malaysia
Email: anissuhaila@utem.edu.my

1. INTRODUCTION

Ion-sensitive field-effect transistors (ISFETs) have emerged as versatile sensors with promising applications spanning environmental monitoring, agriculture, the food industry, and chemical and biosensing [1]–[3]. ISFETs detect signals in the form of voltage or current generated by interactions at the dielectric-electrolyte interface. Their primary application, pH sensing, is particularly noteworthy, enabling precise pH measurements in chemical and biological solutions. Recent advances in ISFET technology have led to the development of flexible potentiometric pH sensors suitable for wearable systems, broadening their utility [4]–[6]. Additionally, ISFETs exhibit great potential for biosensing applications, with notable progress made in this field in recent years. They can accurately identify various target analytes in diverse solutions.

ISFET sensors have garnered significant attention for their potential to enhance sensitivity across diverse applications, particularly in biomedical and environmental monitoring. The Nernst limit for ISFETs is 59 mV/pH at 25 °C, motivating research to boost sensor sensitivity [7]. The effectiveness of an ISFET is substantially influenced by sensitivity, which is evaluated as the percentage of voltage shift per pH rise. Sensing membrane characteristics, gate structure, and device geometry significantly affect performance [8], [9].

Nevertheless, computer simulation is required for design and optimization due to the complex and non-linear aspects of ISFET functioning. Moreover, understanding how different high-k dielectric materials affect sensitivity is essential for ISFETs to reach their full potential.

Recent studies have delved into device manufacturing, architecture, sensing film materials, and modelling of ion-selective metal-oxide-semiconductor field-effect transistor (FET) based pH sensors [10]. Counter-ions have emerged as crucial in enhancing pH sensitivity [11]. Various simulation methodologies have contributed to the understanding and advancement of ISFETs for pH sensing applications [12], [13]. Prominent high-k materials used in ISFET simulations include silicon dioxide (SiO_2) and tantalum pentoxide (Ta_2O_5) [14]. Investigations employing the Gouy-Chapman-Stern model have aimed to enhance ISFET sensitivity and stability by introducing a stern layer directly to the electrolyte of the ISFET sensing layer [15]. Using these models, the study mostly explored high-k materials [16], [17]. Additionally, titanium dioxide (TiO_2) has garnered attention as a pH-responsive gate oxide in ISFETs, exhibiting high sensitivity with an average S1 (av) value of 95 µA/pH [18]. Other high-k materials investigated include hafnium (IV) oxide (HfO_2), Ta_2O_5, zirconium dioxide (ZrO_2), aluminium oxide (Al_2O_3), and silicon nitride (Si_3N_4), each contributing to the Nernst equation differently [19], [20].

In light of this, our paper proposes to employ Silvaco technology computer-aided design (TCAD) simulation to assess ISFET susceptibility to pH changes. This research will investigate the impact of gate channel length and sensing membrane thickness on the sensitivity of ISFETs manufactured using various high-k materials, including TiO_2, HfO_2, Ta_2O_5, Al_2O_3, and Si_3N_4. Our goal is to uncover the mechanisms governing ISFET sensitivity and identify optimal values for gate channel length and sensing membrane thickness to optimize ISFET sensitivity.

2. METHOD

2.1. Device structure

Silvaco TCAD, a popular commercial software program for modelling semiconductor devices, was utilized for the simulation. The simulation was carried out for a typical ISFET architecture, with the gate channel length, sensing membrane thickness, and high-k materials varied, as depicted in Figure 1. Silvaco ATHENA, a software for modelling processes, was used to model the structure of the device and its constituent layers. Then, we used Silvaco ATLAS to examine the device's performance by numerically solving the device's equations. These equations include Poisson's, continuity, and carrier transport equations [21].

The structure of an ISFET device, including a silicon substrate, a SiO_2 layer, an electrolyte and a sensing membrane using ATHENA, is depicted in Figure 2. The electrolyte can be defined according to the user's specifications, and this description aligns with the existing literature [22]. High-k materials for sensing membranes, such as Al_2O_3, HfO_2, Si_3N_4, Ta_2O_5, and TiO_2, were utilized in the simulation. The sensing membrane was p-type doped with boron, while the gate electrode was made of aluminium. Gate channel lengths of 250 nm, 200 nm, and 50 nm were employed, with varying sensing membrane thicknesses of 3 nm, 10 nm, and 20 nm. The ISFETs sensitivity to pH changes was evaluated by adjusting the pH of the solution from 2 to 12 and measuring the drain current (I_D). The sensitivity was determined by calculating the alteration in I_D in response to a unit change in pH. The impact of gate channel length and sensing membrane thickness on ISFET sensitivity was investigated.

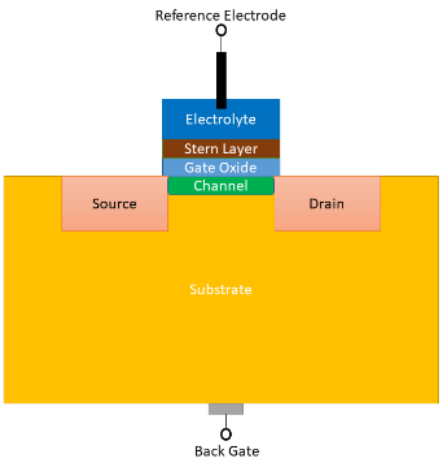

Figure 1. Schematic structure of ISFET

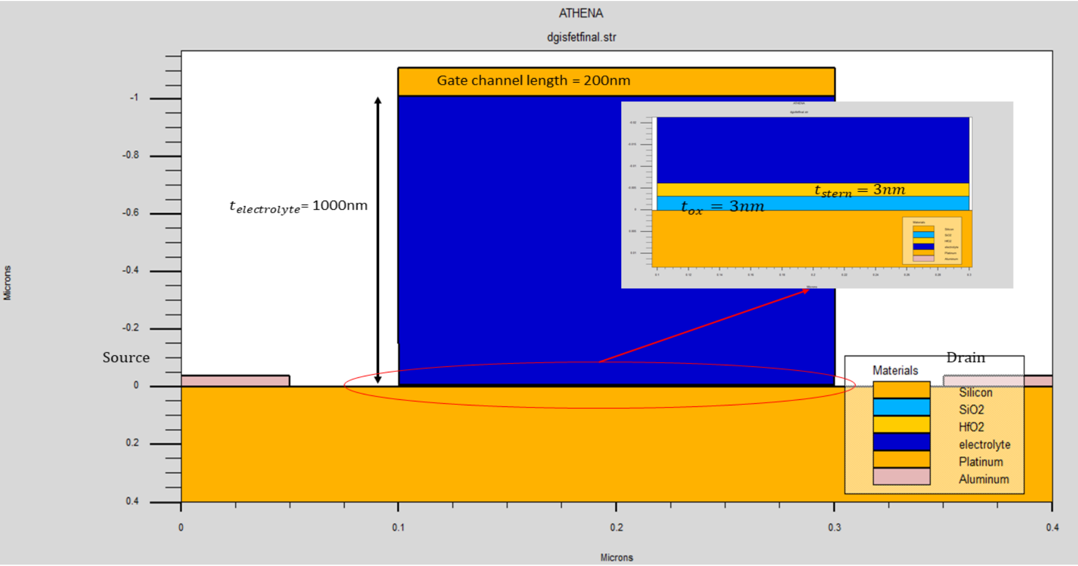

Figure 2. TCAD simulation of ISFET ATHENA structure

2.2. Mathematical models

The ISFETs exhibits sensitivity towards variations in pH levels due to chemical interactions between the gate dielectric of the ISFET and the surrounding liquid, generating a substantial surface charge density. A generic method is currently being developed to strengthen this connection chemically and mathematically. When an insulator is employed as the sensing membrane, the surface of the membrane will experience an accumulation of ions from the electrolyte solution. The concentration of these ions will exhibit a direct proportionality to the pH of the solution. The determination of the surface potential (ψo) is influenced by the binding of hydrogen ions (H+) at the interface between the electrolyte solution and the insulator sites, leading to a substantial impact. In order to achieve maximum efficiency, an insulator should possess favourable reactivity within the specific pH range of relevance while also demonstrating pH sensitivity across a broad spectrum of pH scales. This strategy aims to thoroughly comprehend the chemical and mathematical elements associated with the pH sensitivity of ISFETs, enabling advanced and adaptable sensing methodologies. Various mathematical models simulate the ISFETs behaviour using Silvaco TCAD software. These models describe the electrical properties and behaviour of the ISFET device. The mathematical model used for ISFET simulation is represented by the equations.

The equation for the gate voltage (V_G) can be derived by combining the flat-band voltage (V_{FB}), the contribution from the charge in the depletion region $\frac{qN_A X_{d,T}}{C_{ox}}$, and the contribution from the potential drop across the depletion region $\frac{qN_A (X_{d,T})^2}{2\varepsilon_s}$.

$$V_G = V_{FB} + \frac{qN_A X_{d,T}}{C_{ox}} + \frac{qN_A (X_{d,T})^2}{2\varepsilon_s} \quad (1)$$

This context uses the notations V_G represents the V_G, V_{FB} for the V_{FB}, q for the electronic charge, N_A for the doping concentration, X_d for the width of the depletion layer, T denotes the temperature, cox for the insulator capacitance per unit area (C_{ox}) , and ε_s for the semiconductor permittivity.

$$X_d = \sqrt{\frac{2\varepsilon_s (V_G - V_{FB})}{qN_A}} \quad (2)$$

The ISFET threshold voltage (V_{th}) is calculated as the sum of the V_{FB}, the body effect coefficient (γs) multiplied by the square root of twice the elementary charge (q) multiplied by the effective channel charge concentration (N_{eff}) and the ψo, and the product of the q, N_{eff}, and ψ_o divided by the oxide C_{ox}. It can be stated mathematically as (3).

$$V_{th} = V_{FB} + \gamma s * \left(\sqrt{2qN_{eff} * \psi o}\right) + \frac{(qN_{eff} * \psi o)}{C_{ox}} \quad (3)$$

This mathematical model considers the contributions of the V_{FB}, γs, ψo, and oxide capacitance to predict the ISFET device's V_{th} accurately. By utilizing this model in the Silvaco TCAD simulation, researchers can gain valuable insights into the behaviour of the ISFET in response to pH variations, enabling the advancement of pH sensing applications.

$$\psi_o = \frac{kT}{q} ln \frac{aH^+_{bulk}}{aH^+_{surface}} \tag{4}$$

In the given context, "q" denotes elementary charges, whereas "k" indicates the Boltzmann constant. The variable "a" represents the proton activity at the interface between the gate dielectric and electrolyte and within the electrolyte. Therefore, it can be shown from (3) and (4) that the change in V_{th} for traditional ISFETs is governed by the following expression.

$$V^T_{th} = -\Delta \tag{5}$$

Figure 2 depicts a setup of an ISFET. In a traditional MOSFET, the gate is replaced with a fluid electrolyte. The equations that regulate the behaviour of cations and anions in an electrolyte at equilibrium resemble those that describe the movement of holes and electrons in a semiconductor. The equations mentioned earlier are utilized in developing a theoretical framework to describe electrolytes behaviour. Therefore, it can be deduced that an undoped semiconductor with a bandgap of zero (thus, satisfying the condition n.p= N_cN_v), a constant permittivity ($\epsilon_{el} \approx 80\epsilon 0$), and an adequate density of states (1:1) is classified as a monovalent symmetric (1:1) electrolyte.

$$N_c = N_v = \begin{Bmatrix} 10^{-3} \cdot\ N_{AV}(c_0 + cH_B), & for\ pH_B \leq 7 \\ 10^{-3} \cdot\ N_{AV}\left(c_0 + \frac{10^{-4}}{cH\ \ _B}\right) & for\ pH_B > 7 \end{Bmatrix} \tag{6}$$

The variables N_c and N_v are expressed in units of cm^{-3}, N_{AV} which means Avogadro's number is equal to 6.02214×10^{23} mol^{-1}. The variable c_0 donates the molar concentration of salt ions (M=mol/l) in the bulk of the solution. On the other hand, $cH_B=[H^+_B]=10^{-pHB}$ represents the hydrogen concentration in the bulk of the solution normalized to 1 M.

The determination of the ISFETs sensitivity to variations in pH was accomplished through the examination and analysis of the simulation outcomes. The sensitivity was determined using the (7):

$$\text{Sensitivity} = \left(\frac{\Delta VpH}{\Delta pH}\right) \times 100\% \tag{7}$$

where ΔVpH is the change in voltage with a change in pH and ΔpH is the change in pH.

3. RESULTS AND DISCUSSION

In this section, the results of the comparison between different high-k materials as sensing membranes for ISFET will be presented. The sensing membranes employed in this study consist of Al_2O_3, HfO_2, Si_3N_4, Ta_2O_5, and TiO_2. Table 1 shows the simulation parameters utilized in the TCAD software. Table 2 displays the essential parameters required for validation and simulation. These values can be derived from the data presented in the previous literature sources [8], [23], [24].

Table 1. The parameters of TCAD for ISFET [8], [23], [24]

Parameter	Value	Unit
t_{stern}	3, 10, 20	nm
T	300	K
k	1.380649×10^{-23}	J/K
$t_{electrolyte}$	1000	nm
t_{ox}	3	nm
Electrolyte permittivity	80	-
S/D doping	10^{20}	cm^{-3}
Channel length	50, 200, 250	nm
Electrolyte concentration	10^{-3}	Mol/L
V_{DS}	10	mV
S/D length	50	nm

Table 2. Parameters of high-k materials used in TCAD simulation [8], [23], [24]

Material	Bandgap (E_{g300})	Permittivity	Effective conduction insufficient (N_c)	Effective valence band (N_v)
Al_2O_3	8	8	6.7×10^{22}	6.7×10^{22}
HfO_2	5.8	25	1.3×10^{22}	1.6×10^{22}
Si_3N_4	5.3	7	3.1×10^{22}	1.9×10^{22}
Ta_2O_5	22	4.4	1.6×10^{22}	12.2×10^{22}
TiO_2	3.5	80	1.3×10^{22}	1.6×10^{22}

The simulation results provided in Figure 3(a) to 7(i), Figures 6(a) to 7(i) result from an investigation into the electrostatic behaviour of an ISFET device. The provided figures depict the correlation between the I_D and the reference gate voltage (V_{Ref}) across a range of pH values from pH 2 to 12. The simulations were conducted considering various combinations of gate channel lengths (50 nm, 200 nm, and 250 nm) and thicknesses of the different sensing membranes (3 nm, 10 nm, and 20 nm).

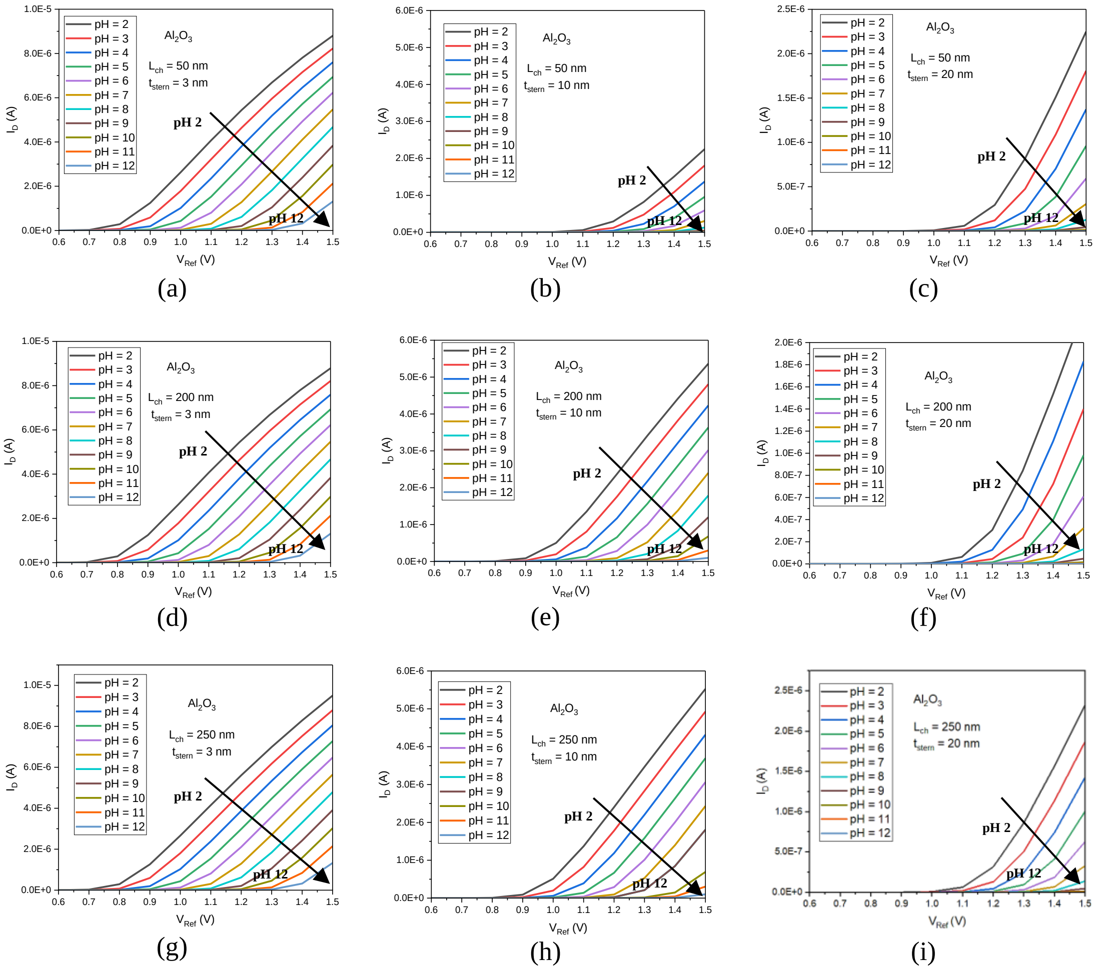

Figure 3. The I_D was analyzed in relation to the V_{Ref} at various pH values ranging from 2 to 12 for different combinations of gate channel lengths and thicknesses of the sensing membrane, specifically Al_2O_3, the following configurations were considered: (a) gate length=50 nm and thickness of Al_2O_3=3 nm; (b) gate length=50 nm and thickness of Al_2O_3=10 nm; (c) gate length=50 nm and thickness of Al_2O_3=20 nm; (d) gate length=200 nm and thickness of Al_2O_3=3 nm; (e) gate length=200 nm and thickness of Al_2O_3=10 nm; (f) gate length=200 nm and thickness of Al_2O_3=20 nm; (g) gate length=250 nm and thickness of Al_2O_3=3 nm; (h) gate length=250 nm and thickness of Al_2O_3=10 nm; and (i) gate length=250 nm and thickness of Al_2O_3=20 nm

The transfer curves for each pH value show the I_D-V_{Ref} relationship. A sensitivity analysis of the ISFET device to changes in pH levels can be conducted by analyzing the transfer characteristics. Acidic conditions show a positive link between I_D and V_{Ref}. Lower pH values show the I_D non-linear response to V_{Ref}

changes. At alkaline pH levels, the I_D decreases compared to the V_{Ref}. When the V_{Ref} changes, the I_D behaves nonlinearly at pH values [25].

The variations in gate channel length and sensing membrane thickness enable an analysis of their effect on the device's pH sensitivity. These simulation results provide significant insight into the electrostatic behaviour of the ISFET device, demonstrating its response to changes in pH under various experimental conditions. The size of the gate channel is essential when designing and analyzing FETs. It is the distance between the source and the drain. When the gate channel's length decreases, the channel's pH sensitivity changes. The shortened channel length enables a greater electric field and sensitivity to pH-induced variations in ψo. There appears to be a correlation between increased gate channel length and less susceptibility to pH changes. The longer the channel, the lower the electric field and the exposure to pH-induced changes in ψo [26], [27].

On the other hand, a thinner sensor membrane can increase its sensitivity to changes in pH. In reaction to changes in pH, the thinner membrane has a shorter response time and greater sensitivity to changes in ψo. A potential consequence of using a thicker sensing membrane is a reduction in sensitivity toward changes in pH levels. The thicker membrane may slow the reaction time and make it less sensitive to changes in the ψo caused by pH changes. By examining the transfer characteristics at different pH levels, researchers can better understand the device's performance and optimize its design for pH sensing applications [28], [29].

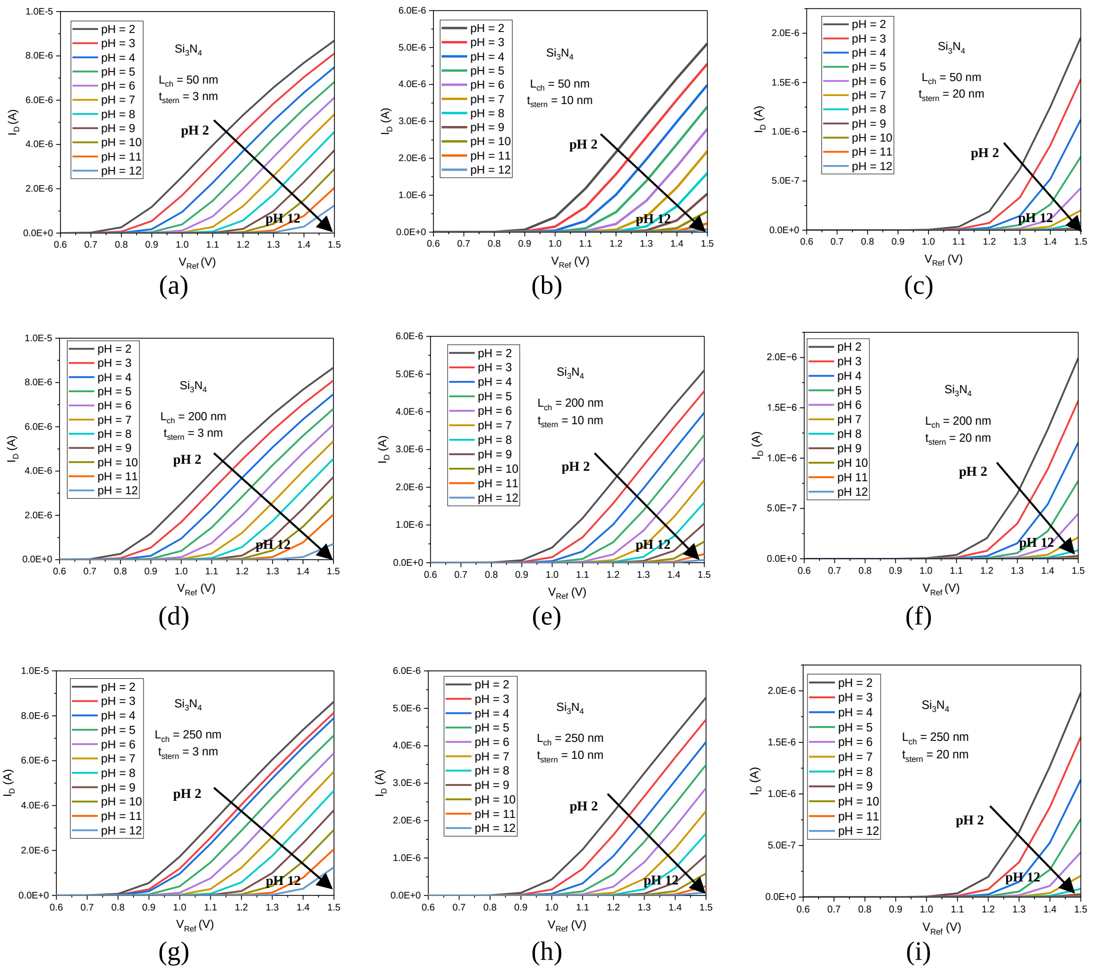

Figure 4. The I_D was analyzed in relation to the V_{Ref} at various pH values ranging from 2 to 12 for different combinations of gate channel lengths and thicknesses of the sensing membrane, specifically Si_3N_4, the following configurations were considered: (a) gate length=50 nm and thickness of Si_3N_4=3 nm; (b) gate length=50 nm and thickness of Si_3N_4=10 nm; (c) gate length=50 nm and thickness of Si_3N_4=20 nm; (d) gate length=200 nm and thickness of Si_3N_4=3 nm; (e) gate length=200 nm and thickness of Si_3N_4=10 nm; (f) gate length=200 nm and thickness of Si_3N_4=20 nm; (g) gate length=250 nm and thickness of Si_3N_4=3 nm; (h) gate length=250 nm and thickness of Si_3N_4=10 nm; and (i) gate length=250 nm and thickness of Si_3N_4=20 nm

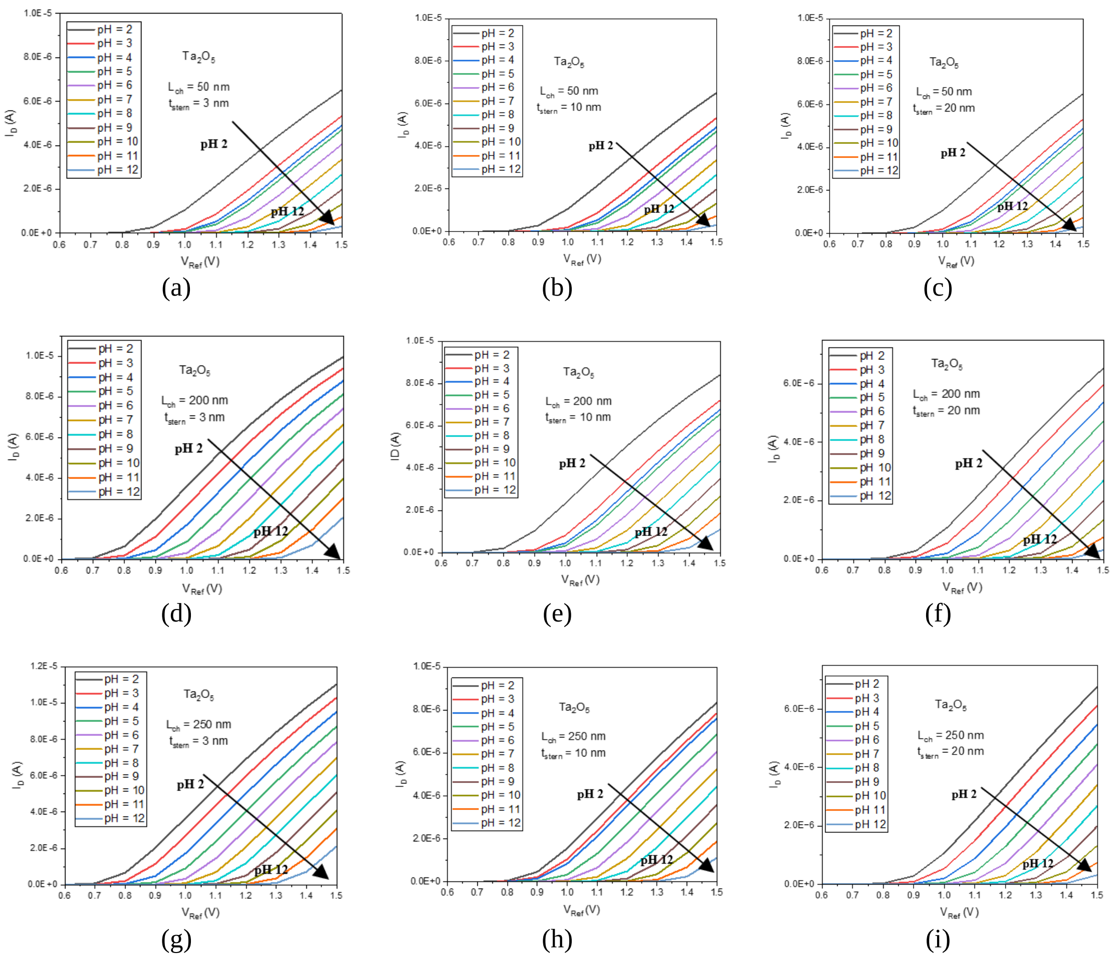

Figure 5. The I_D was analyzed in relation to the V_{Ref} at various pH values ranging from 2 to 12 for different combinations of gate channel lengths and thicknesses of the sensing membrane, specifically Ta_2O_5, the following configurations were considered: (a) gate length=50 nm and thickness of Ta_2O_5=3 nm; (b) gate length=50 nm and thickness of Ta_2O_5=10 nm; (c) gate length=50 nm and thickness of Ta_2O_5=20 nm; (d) gate length=200 nm and thickness of Ta_2O_5=3 nm; (e) gate length=200 nm and thickness of Ta_2O_5=10 nm; (f) gate length=200 nm and thickness of Ta_2O_5=20 nm; (g) gate length=250 nm and thickness of Ta_2O_5=3 nm; (h) gate length=250 nm and thickness of Ta_2O_5=10 nm; and (i) gate length=250 nm and thickness of Ta_2O_5=20 nm

The simulation results indicated that the ISFET exhibited the highest average sensitivity for various high-k materials when the gate channel length was 200 nm, and the thickness of the sensing membrane was 3 nm. A gate channel length of 50 nm and 3 nm thickness sensing membrane has some benefits, including shorter response times and increased electron mobility. Nevertheless, it presents some obstacles. The more transient channel length can increase leakage currents and greater susceptibility to short-channel effects, impacting the device's performance and sensitivity. There will also be issues with real-time fabrication. In this study, the simulation results have demonstrated that the ISFET exhibits enhanced sensitivity when utilizing a 200 nm gate channel length and a 3 nm sensing membrane thickness. These specific dimensions have been found to strike a more favourable balance of electrical properties, leading to improved performance of the ISFET.

Figure 8 illustrates a positive correlation between higher pH levels and increased V_{th}. The V_{th} of sensing membranes is determined by a gate channel length of 200 nm and a sensing membrane thickness of 3 nm. Changes in pH levels can modify the V_{th} of an ISFET. The difference in observed shift voltage suggests that pH levels impact the charge distribution and potential above the gate insulator. The voltage shift at the threshold remains constant across all pH levels during the transition from a high to a low pH. When using pH buffer solutions with a higher concentration of counter-ions, the sensor's sensitivity increases significantly and can potentially exceed the Nernst limit. The V_{th} of pH-sensitive ISFETs increases progressively due to a physical model that explains V_{th} drift. Variations in the pH of the solution can affect the solution gate interface potential of the ISFET, resulting in a change in the threshold shift. So, when making and using ISFET devices for pH reading, it is essential to consider the pH value of the tested chemical [19], [24].

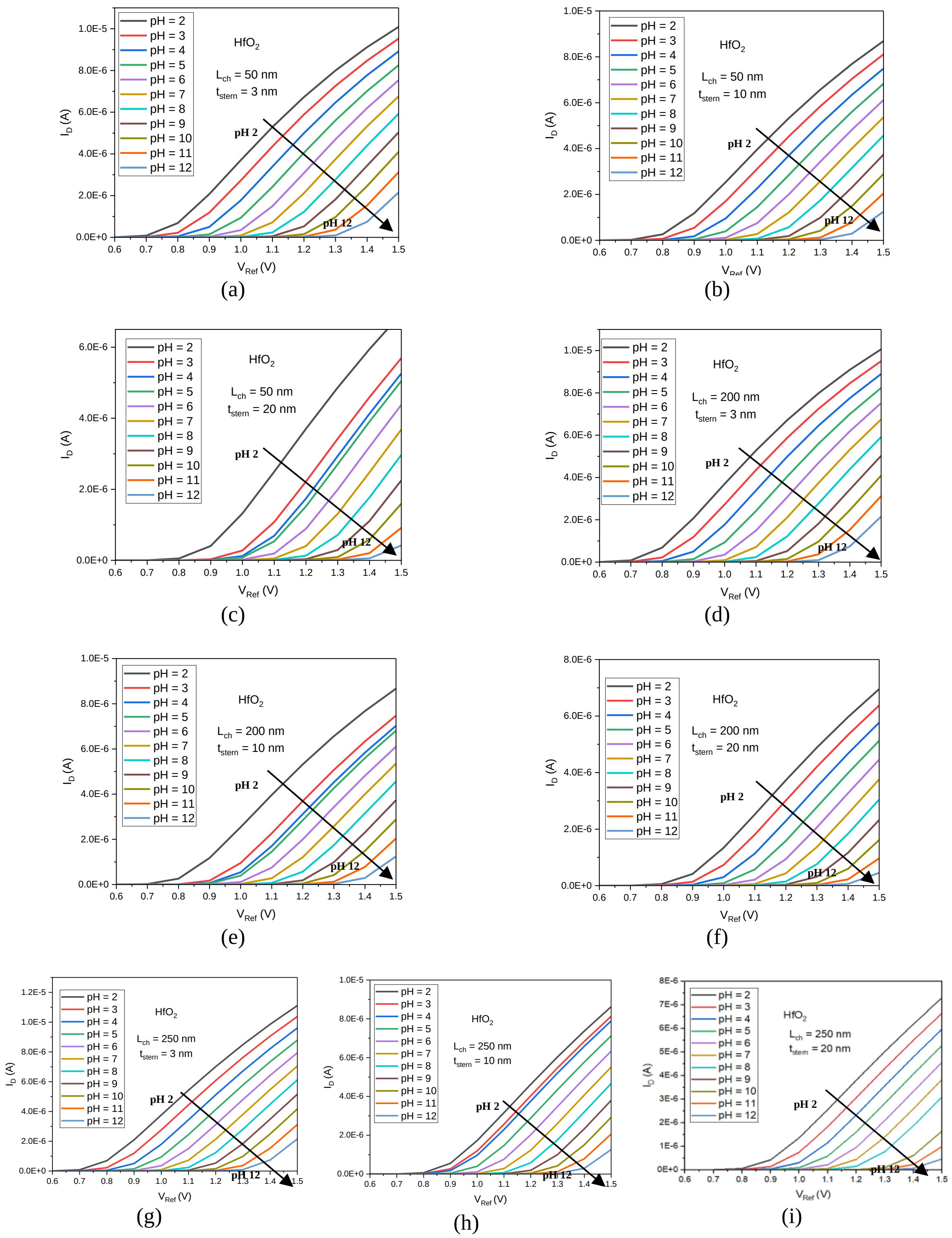

Figure 6. The I_D was analyzed in relation to the V_{Ref} at various pH values ranging from 2 to 12 for different combinations of gate channel lengths and thicknesses of the sensing membrane, specifically HfO_2, the following configurations were considered: (a) gate length=50 nm and thickness of HfO_2=3 nm; (b) gate length=50 nm and thickness of HfO_2=10 nm; (c) gate length=50 nm and thickness of HfO_2=20 nm; (d) gate length=200 nm and thickness of HfO_2=3 nm; (e) gate length=200 nm and thickness of HfO_2=10 nm; (f) gate length=200 nm and thickness of HfO_2=20 nm; (g) gate length=250 nm and thickness of HfO_2=3 nm; (h) gate length=250 nm and thickness of HfO_2=10 nm; and (i) gate length=250 nm and thickness of HfO_2=20 nm

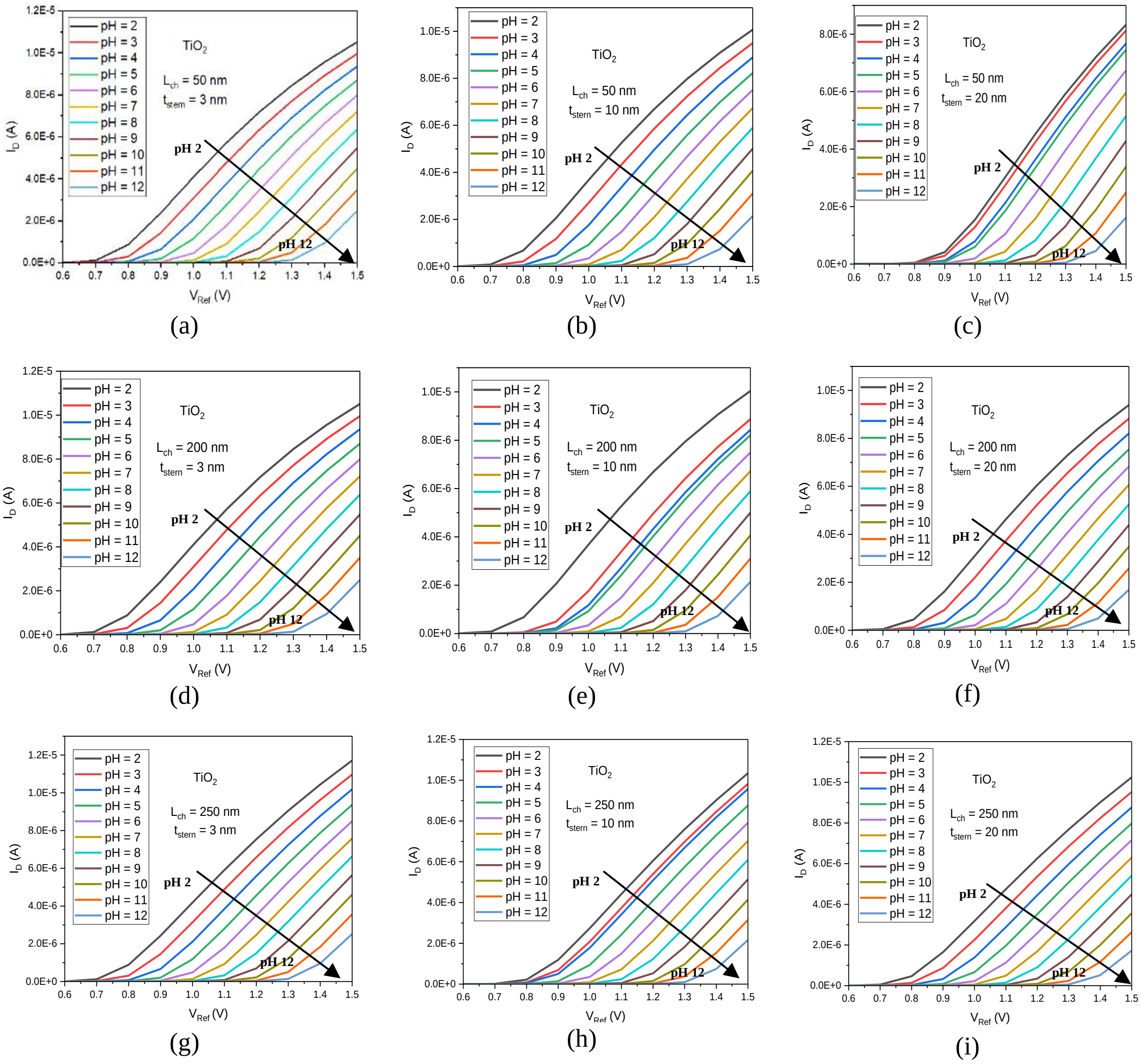

Figure 7. The I_D was analyzed in relation to the V_{Ref} at various pH values ranging from 2 to 12 for different combinations of gate channel lengths and thicknesses of the sensing membrane, specifically TiO_2, the following configurations were considered: (a) gate length=50 nm and thickness of TiO_2=3 nm; (b) gate length=50 nm and thickness of TiO_2=10 nm; (c) gate length=50 nm and thickness of TiO_2=20 nm; (d) gate length=200 nm and thickness of TiO_2=3 nm; (e) gate length=200 nm and thickness of TiO_2=10 nm; (f) gate length=200 nm and thickness of TiO_2=20 nm; (g) gate length=250 nm and thickness of TiO_2=3 nm; (h) gate length=250 nm and thickness of TiO_2=10 nm; and (i) gate length=250 nm and thickness of TiO_2=20 nm

Next, Figure 9 shows the average sensitivity for high-k materials with a Nernst limit of 59.000 mV/pH. As shown, the most contributed one is TiO_2 by 57.9751 mV/pH, and the following two materials are HfO_2 and Ta_2O_5 by 57.4638 and 57.3617 mV/pH, respectively. The lowest is Al_2O_3 by 55.0542 mV/pH. Finally, the average sensitivity of Si_3N_4 is 54.7472 mV/pH because Si_3N_4 is known to be a unique material due to SiOH groups resulting from silicon oxidation. Moreover, the Si_3N_4 surface exhibits additional basic sites formed by primary amine groups, distinguishing it from other materials. In recent studies by Parizi *et al*. [11] it has been discovered that TiO_2 exhibits a significantly higher sensitivity when compared to other high-k materials like HfO_2, Ta_2O_5, and Al_2O_3. The findings of this study are consistent with the results reported in previous articles [5], [11], [24], [30].

Figure 9 presents the average sensitivity of the sensing membrane, calculated using (7), as a function of gate channel length and sensing membrane thickness. The optimal values for achieving high sensitivity in pH sensing were a gate length of 200 nm and a thickness of sensing membrane, 3 nm, based on the highest sensitivity observed from the varied channel lengths and thicknesses. This result is consistent with previous studies. Therefore, it can be concluded that the choice of gate channel length and sensing membrane thickness are crucial factors in optimizing the sensitivity of ISFETs for pH sensing applications.

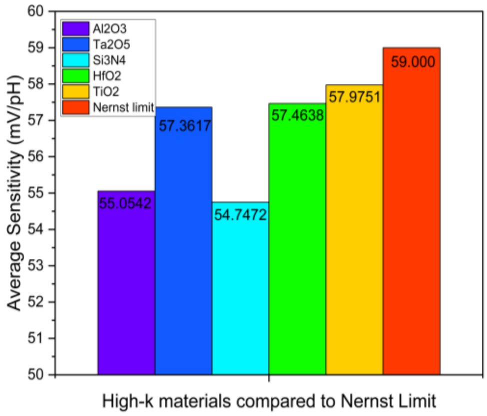

Figure 8. The average sensitivity of different high-k materials as sensing membrane

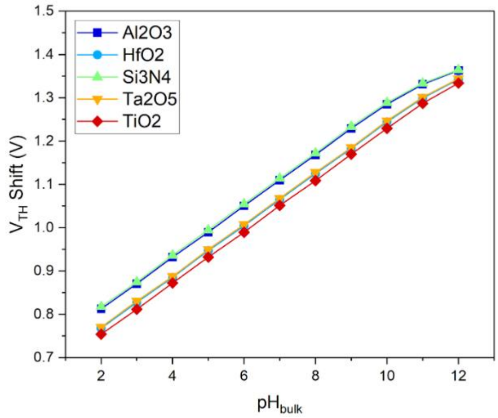

Figure 9. The V_{th} shift was observed in various sensing membranes, each having a gate channel length of 200 nm, and a sensing membrane thickness of 3 nm

4. CONCLUSION

In summary, this study effectively utilized Silvaco software to simulate and evaluate the efficacy of an ISFET biosensor for pH detection in the medical field. The sensor's sensitivity was comprehensively assessed by manipulating channel lengths and sensing membrane thicknesses, considering key factors such as pH value and V_{th}. The study results indicated that TiO_2 demonstrated the most significant sensitivity among the tested materials, with a sensitivity value of 57.98 mV/pH, due to its high sensitivity and stability during measurement. HfO_2, Ta_2O_5, Al_2O_3, and Si_3N_4 followed closely behind in sensitivity. The findings of this study emphasize the potential of ISFET, specifically those incorporating TiO_2 sensing membranes, as reliable and precise pH monitoring systems in biomedical applications. Additionally, this study significantly contributes to improving accuracy and responsiveness in biosensors utilizing ISFET, thereby facilitating progress in chemical detection within the field of biological sciences. The Silvaco software has been recognized as a dependable and economically efficient tool for modelling ISFET-based biosensors, facilitating their design and optimization.

ACKNOWLEDGEMENTS

We express our gratitude to Centre for Research and Innovation Management (CRIM) and Faculty of Electronics and Computer Technology and Engineering (FTKEK), Universiti Teknikal Malaysia Melaka.

REFERENCES

[1] G. Elli *et al.*, "Field-effect transistor-based biosensors for environmental and agricultural monitoring," *Sensors*, vol. 22, no. 11, p. 4178, May 2022, doi: 10.3390/s22114178.
[2] T. C. Ye, S. F. W. M. Hatta, N. Soin, and A. A. B. Sajak, "Modeling and optimization of ISFET microsensor for the use of quality testing in food and pharmaceutical industry," in *Proceedings-2021 IEEE Regional Symposium on Micro and Nanoelectronics*, Aug. 2021, pp. 120–123, doi: 10.1109/RSM52397.2021.9511588.
[3] C. Jimenez-Jorquera, J. Orozco, and A. Baldi, "ISFET based microsensors for environmental monitoring," *Sensors*, vol. 10, no. 1, pp. 61–83, Dec. 2010, doi: 10.3390/s100100061.
[4] Y. Jiang *et al.*, "A high-sensitivity potentiometric 65-nm CMOS ISFET sensor for rapid E. coli screening," *IEEE Transactions on Biomedical Circuits and Systems*, vol. 12, no. 2, pp. 402–415, Apr. 2018, doi: 10.1109/TBCAS.2018.2793861.
[5] L. Jiao and N. Barakat, "Ion-sensitive field effect transistor as a PH sensor," *Journal of Nanoscience and Nanotechnology*, vol. 13, no. 2, pp. 1194–1198, 2013, doi: 10.1166/jnn.2013.6065.
[6] J. H. Jeon and W. J. Cho, "High-performance extended-gate ion-sensitive field-effect transistors with multi-gate structure for transparent, flexible, and wearable biosensors," *Science and Technology of Advanced Materials*, vol. 21, no. 1, pp. 371–378, Jan. 2020, doi: 10.1080/14686996.2020.1775477.
[7] P. Bergveld, "Future applications of ISFETs," *Sensors and Actuators: B. Chemical*, vol. 4, no. 1–2, pp. 125–133, May 1991, doi: 10.1016/0925-4005(91)80187-O.
[8] A. S. M. Zain *et al.*, "Effects of ISFET geometrical parameters on sensing proprieties," *Proceedings of Mechanical Engineering Research Day*, pp. 160–161, 2020.
[9] IEEE Staff, *2019 International Conference on Wireless Technologies, Embedded and Intelligent Systems (WITS)*. IEEE, 2019.
[10] J. Park, H. H. Nguyen, A. Woubit, and M. Kim, "Applications of field-effect transistor (FET)-type biosensors," *Applied Science and Convergence Technology*, vol. 23, no. 2, pp. 61–71, Mar. 2014, doi: 10.5757/asct.2014.23.2.61.
[11] K. B. Parizi, X. Xu, A. Pal, X. Hu, and H. S. P. Wong, "ISFET pH sensitivity: counter-ions play a key role," *Scientific Reports*, vol. 7, no. 1, p. 41305, Feb. 2017, doi: 10.1038/srep41305.

[12] D. Passeri, A. Morozzi, K. Kanxheri, and A. Scorzoni, "Numerical simulation of ISFET structures for biosensing devices with TCAD tools," *BioMedical Engineering Online*, vol. 14, no. 2, p. S3, 2015, doi: 10.1186/1475-925X-14-S2-S3.
[13] N. Choksi, D. Sewake, S. Sinha, R. Mukhiya, and R. Sharma, "Modeling and simulation of ISFET using TCAD tool for various sensing films," 2017.
[14] J. H. Jeon and W. J. Cho, "Ultrasensitive coplanar dual-gate ISFETs for point-of-care biomedical applications," *ACS Omega*, vol. 5, no. 22, pp. 12809–12815, Jun. 2020, doi: 10.1021/acsomega.0c00427.
[15] A. M. Dinar, A. S. M. Zain, F. Salehuddin, M. K. Abdulhameed, M. K. Mohsen, and M. L. Attiah, "Impact of Gouy-Chapman-Stern model on conventional ISFET sensitivity and stability," *Telecommunication Computing Electronics and Control*, vol. 17, no. 6, pp. 2842–2850, Dec. 2019, doi: 10.12928/TELKOMNIKA.v17i6.12838.
[16] P. D. V. D. Wal *et al.*, "High-k dielectrics for use as ISFET gate oxides," in *Proceedings of IEEE Sensors*, 2004, vol. 2, pp. 677–680, doi: 10.1109/icsens.2004.1426257.
[17] S. N. Supardan, Study of high-k dielectrics and their interfaces on semiconductors for device applications. The University of Liverpool (United Kingdom), 2019.
[18] D. L. Harame, L. J. Bousse, J. D. Shott, and J. D. Meindl, "Ion-sensing devices with silicon nitride and borosilicate grlass insulators," *IEEE Transactions on Electron Devices*, vol. 34, no. 8, pp. 1700–1707, Aug. 1987, doi: 10.1109/T-ED.1987.23140.
[19] A. M. Dinar, A. S. M. Zain, and F. Salehuddin, "Comprehensive identification of sensitive and stable ISFET sensing layer high-k gate based on ISFET/electrolyte models," *International Journal of Electrical and Computer Engineering*, vol. 9, no. 2, pp. 926–933, 2019, doi: 10.11591/ijece.v9i2.pp926-933.
[20] H. J. Jang and W. J. Cho, "High performance silicon-on-insulator based ion-sensitive field-effect transistor using high-k stacked oxide sensing membrane," *Applied Physics Letters*, vol. 99, no. 4, Jul. 2011, doi: 10.1063/1.3619831.
[21] "ATLAS user's manual: device simulation software," 2004.
[22] A. M. Dinar, A. S. M. Zain, F. Salehuddin, M. L. Attiah, M. K. Abdulhameed, and M. K. Mohsen, "Modeling and simulation of electrolyte pH change in conventional ISFET using commercial Silvaco TCAD," *IOP Conference Series: Materials Science and Engineering*, vol. 518, no. 4, p. 042020, May 2019, doi: 10.1088/1757-899X/518/4/042020.
[23] T. M. Abdolkader, A. G. Alahdal, A. Shaker, and W. Fikry, "ISFET pH-sensor sensitivity extraction using conventional MOSFET simulation tools," *International Journal of Chemical Engineering and Applications*, vol. 6, no. 5, pp. 346–351, Oct. 2015, doi: 10.7763/ijcea.2015.v6.507.
[24] A. M. Dinar, A. S. M. Zain, F. Salehuddin, M. K. Mohsen, M. L. Attiah, and M. K. Abdulhameed, "Performance analysis of high-k materials as stern layer in ion-sensitive field effect transistor using commercial TCAD," *Telecommunication Computing Electronics and Control*, vol. 17, no. 6, pp. 2867–2876, Dec. 2019, doi: 10.12928/TELKOMNIKA.v17i6.12852.
[25] S. J. Young, Y. J. Chu, and Y. L. Chen, "Enhancing pH Sensors performance of ZnO nanorods with Au nanoparticles Adsorption," *IEEE Sensors Journal*, vol. 21, no. 12, pp. 13068–13073, Jun. 2021, doi: 10.1109/JSEN.2021.3062857.
[26] X. Ma, R. Peng, W. Mao, Y. Lin, and H. Yu, "Recent advances in ion-sensitive field-effect transistors for biosensing applications," *Electrochemical Science Advances*, vol. 3, no. 3, Jun. 2023, doi: 10.1002/elsa.202100163.
[27] H. Liu *et al.*, "Ultrafast, sensitive, and portable detection of COVID-19 IgG using flexible organic electrochemical transistors," *Science Advances*, vol. 7, no. 38, 2021, doi: 10.1126/sciadv.abg8387.
[28] Y. Chang *et al.*, "First decade of interfacial iontronic sensing: from droplet sensors to artificial skins," *Advanced Materials*, vol. 33, no. 7, Feb. 2021, doi: 10.1002/adma.202003464.
[29] M. Venkatesan *et al.*, "Evolution of electrospun nanofibers fluorescent and colorimetric sensors for environmental toxicants, pH, temperature, and cancer cells–a review with insights on applications," *Chemical Engineering Journal*, vol. 397, p. 125431, Oct. 2020, doi: 10.1016/j.cej.2020.125431.
[30] J. C. Chou and L. P. Liao, "Study on pH at the point of zero charge of TiO2 pH ion-sensitive field effect transistor made by the sputtering method," *Thin Solid Films*, vol. 476, no. 1, pp. 157–161, Apr. 2005, doi: 10.1016/j.tsf.2004.09.061.

BIOGRAPHIES OF AUTHORS

Nur Afiqah Hani Senin in 2022, she obtained a Bachelor's degree Electronic Engineering from Universiti Teknikal Malaysia Melaka. She is now pursuing a Master's degree in Microelectronics and Nanotechnology. Her research is focused on ISFET. She can be contacted at email: m022210004@student.utem.edu.my.

Anis Suhaila Mohd Zain received the B.Eng. degree in Electrical, Electronic, and System Engineering and M.Sc. degree in Microelectronics from Universiti Kebangsaan Malaysia (UKM), in 2000 and 2001 respectively. She received the Ph.D. degree in Electronics and Electrical Engineering from University of Glasgow (UK, Scotland), Malaysia in 2013. She joined Universiti Teknikal Malaysia Melaka (UTeM) in February 2002 as a lecturer and is currently a senior lecturer at the Faculty of Electronic and Computer Engineering (FKEKK), UTeM. Her research interest includes nanoscale device design and simulation, nanotechnology variability and reliability of emerging technology devices, and IC design for biomedical applications. She can be contacted at email: anissuhaila@utem.edu.my.

Fauziyah Salehuddin holds the position of Associate Professor at Universiti Teknikal Malaysia Melaka. She got a Doctor of Philosophy degree from Universiti Tenaga Nasional. She is employed at the Faculty of Electronic and Computer Engineering (FKEKK), UTeM. She is interested in statistical modelling, variability, and CMOS design. She can be contacted at email: fauziyah@utem.edu.my.

Hazura Haroon currently works at the Department of Electronics and Computer Engineering, Universiti Teknikal Malaysia Melaka (UTeM). She does research in mechanical engineering, electrical engineering and electronic engineering. Their current project is modelling, design, and optimization of optical and semiconductor devices. She can be contacted at email: hazura@utem.edu.my.

Ahmed Musa Dinar currently a lecturer at the Department of Computer Engineering, University of Technology, Baghdad, Iraq. He received a B.Sc. degree in Computer and Software Engineering from Al-Mustansiriya University, Iraq, in 2007 and M.Sc. degree in Computer Engineering from University of Technology, Iraq in 2014. He obtained his Ph.D. in Computer Engineering from UTeM, Malaysia in 2020. His research interests mainly focus on sensors and computing tools for biomedical applications. He can be contacted at email: ahmed.m.dinar@uotechnology.edu.iq.

Norwahidah Abdul Karim lecturer at Department of Biochemistry, Universiti Kebangsaan Malaysia Medical Centre since 2008. Graduated from UKM with Bachelor of Biomedical Sciences (Hons.) in 2000 and graduated with Ph.D. in Medical Biochemistry in 2007. Actively involved in teaching undergraduate and postgraduate medical program. The pioneer of molecular research in autism-related-mitochondria abnormalities in Malaysia and was trained under Oroboros O2k-Workshop on High-Resolution FluoRespirometry (HRFR), IOC122 at Schroecken, Austria on Jun 2016. Her research area includes the elucidation of underlying mechanism of autism spectrum disorder (ASD) by proteomic and genomics study using autism lymphoblast cells, elucidation of mitochondrial abnormalities and oxidative stress in autism lymphoblast cells and intervention with natural product in-vitro such as vit E, tocotrienol-rich fraction, and honey. She can be contacted at email: norwahidah@ukm.edu.my.